

Mineralogy and Geochemistry of Peridotites of Noorabad Ophiolite as Part of Kermanshah Ophiolite (Lorestan Province, West Iran)



Masoud Kiani, Nima Nezafati*, Mansour Vosoughi and Abediniand AliSolgi
Department of Geology & Geophysics, Islamic Azad University, Science
and Research Branch, Tehran- 1477893855, Iran*Email:kianigemology@gmail.com
Received: April 11, 2018; Revised: March 15, 2019; Accepted: March 30, 2019

Abstract : The Kermanshah ophiolite, a part of outer ophiolites of Zagrosbelt, located in the high Zagros zone (Zagros Thrust), trending NW – SE, stretching 230 km in length and 30-60 km in width, west of Iran is a part of the Neo-Tethys oceanic crust, that was obducted on the margin of the Iranian Plate. The peridotites of the ophiolite in Noorabad area include dunites, harzburgites and lherzolites, which are depleted in incompatible elements along with a negative slope of incompatible light elements to 'high field strength elements' (HFSE). These rocks in normalized chondrite show depletion in REE with a negative slope of HFSE to 'large ion lithophile elements' (LILE). The melting percentage in studied peridotites indicates a high f_o_2 than MORB, which indicates that the peridotites of this region are related to the peridotites of the Supra Subduction Zone (SSZ) in the Neo-Tethys Ocean.

Keyword: Kermanshah ophiolite, Zagrosbelt, Peridotites, Supra Subduction Zone.

Zagros ophiolite belt of Iran, a part of the Eastern Mediterranean ophiolite belt shows characteristics of ophiolites associated with Supra Subduction Zone (SSZ, Fig. 1, Shafaii Moghadam and Stern, 2011; Dilek *et al.*, 2007; Parlak *et al.*, 2006; Hébert *et al.*, 2003; Malpas *et al.*, 2003; Hassanipak and Ghazi, 2000; Arvin, 1990; Robinson and Malpas, 1990; Hébert *et al.*, 1989; Pearce *et al.*, 1984 and 1981; Kiani, 2011; Kiani *et al.*, 2015 ; Tahmasebi *et al.*, 2016; and Shafaii Moghadam *et al.*, 2012).

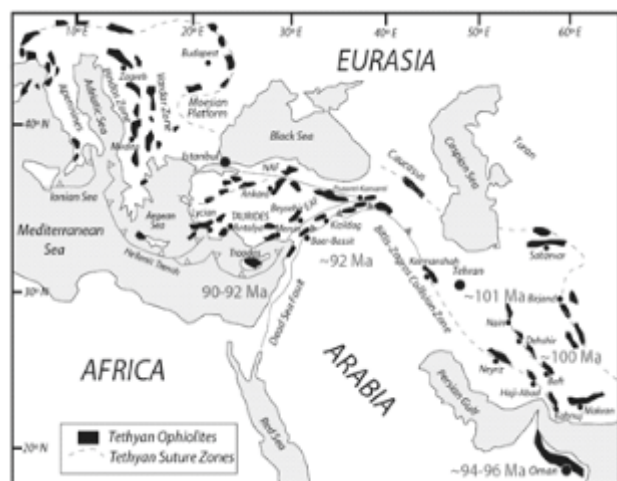


Fig.1. Simplified tectonic map of the eastern Mediterranean-Zagros region showing the distribution of Neotethyan ophiolites and suture zones (modified after Dilek *et al.*, 2007; Shafaii Moghadam *et al.*, 2013). The U-Pb zircon ages for Troodos ophiolite trondhjemites and gabbro are from Mukasa and Ludden (1987), for Kizildag from Dilek and Thy (2009), for Oman from Warren *et al.* (2005) and Goodenough *et al.* (2010), and for the Nain-Dehshir ophiolites are from Shafaii Moghadam *et al.* (2013).

The belt is divided into two groups: 'outer-' and 'inner Zagrosophiolites' (Stocklin, 1977). The former includes the Kermanshah, Neyriz and Hajiabad ophiolites (Shafaii Moghadam and Stern, 2011) with NW-SE trend as a part of the 3,000 km ophiolite belt stretching from Cyprus to Oman (Dilek and Delaloy, 1992) and the latter occurs around central Iran. The Kermanshah ophiolite belt is 230 km long and 30-60 km wide (Fig. 2) located in the western Iran is part of the Neo-Tethys oceanic crust that has been obducted on the margin of the Iran Plate (Kiani, 2011). The present study deals with field geological observations, mineralogy and geochemistry of peridotites of Noorabad ophiolite exposed in the southern part of Kermanshah ophiolite.

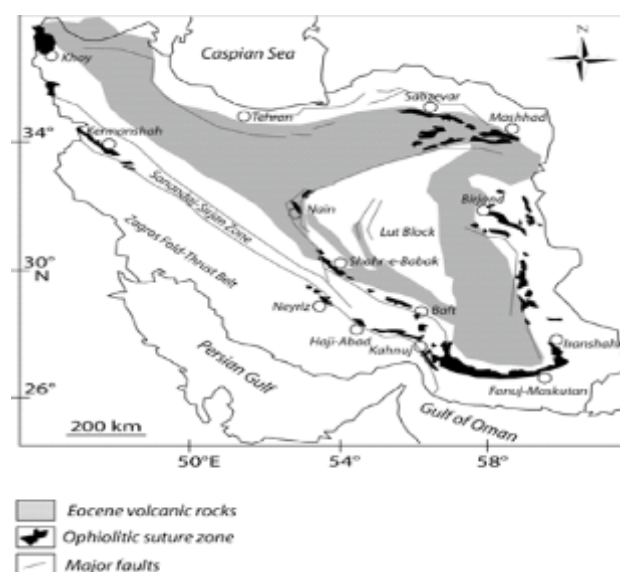


Fig. 2: Distribution ophiolites map of Iran.

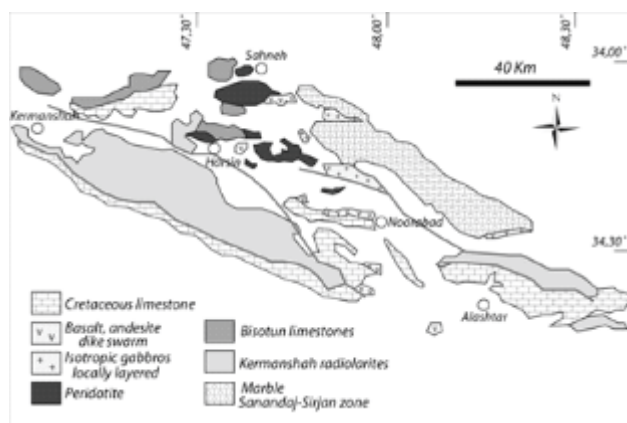


Fig. 3: Geology Map of Noorabad ophiolite .

Regional geology

The Kermanshah ophiolite complex is located in the high Zagros zone (thrust Zagros, Fig. 3) with NW-SE trend (Kiani, 2011). The zone is located between the folded Zagros and Sanandaj-Sirjan Zones. The rocks consist of Bisotun limestones, radiolarites and ophiolites, thrust on folded Zagros (Ghazi and Hassanipak 1999; Agard *et al.*, 2005; Kiani *et al.*, 2015; Tahmasebi *et al.*, 2016). The zone was formed by the collision of the Eurasian continent with Africa in Iaramine. The ophiolite complex in this zone consists of serpentinized peridotites, layered gabbros,

isotropic gabbros, a complex of sheet dikes, basalts and sedimentary rocks like radiolarite and pelagic limes of Miocene times (Kiani, 2011). Sanandaj-Sirjan zone, located in the north and northeast of study area comprises Jurassic-Cretaceous limestones, which have been metamorphosed into marble. Also, in the south and southwest of the studied area, there is a Zagros zone that includes the strongly folded Cretaceous limestones and Bakhtiari conglomerate (Fig. 3). The peridotitic rocks occur in eastern Noorabad, the largest volume of all the igneous rocks in the ophiolites complex of Kermanshah. These rocks outcrop in small and large masses, the largest located in the east of Haft Cheshme, 35 km off the Noorabad-Harsin road (Fig. 3), pelagic limes are crushed and altered and vary in colour from green to gray. The peridotites of the region include: dunites, harzburgites and lherzolites.

Analytical Methods

Fifteen samples from less altered peridotites, were collected for petrographical observation, to determine the concentration of major- and minor elements and Rare Earth Elements (REE). Two samples of dunites, four of harzburgites and three of lherzolites were selected for geochemical analysis for major elements using (ICP-OES), and Minor Elements and REE using of (ICP-MS), at Laboratory of LABWEST, Australia (Table 1).

Table 1 . Whole-rock major, trace and rare earth element (REE) analysis of representative rock samples from study area rocks.

Rock type	Dunite	Dunite	Harzburgite	Harzburgite	Harzburgite	Harzburgite	Lherzolite	Lherzolite	Lherzolite
Sample	NK-06	NK-14	NK-04	NK-31	NK-36	S-01	S-02	S-07	NK-05
SiO ₂	40.43	39.70	40.36	41.34	39.82	40.30	39.46	40.34	41.65
TiO ₂	0.01	0.01	0.01	0.01	0.01	0.01	0.04	0.03	0.01
Al ₂ O ₃	0.01	0.49	0.65	0.72	0.45	0.95	2.43	1.71	1.91
Fe ₂ O ₃	6.69	7.66	9.20	6.98	7.81	6.82	6.88	8.28	6.91
MnO	0.09	0.12	0.14	0.09	0.12	0.07	0.11	0.12	0.10
MgO	45.45	44.63	41.35	43.50	42.95	43.78	43.42	42.36	42.67
CaO	0.12	0.16	0.43	0.04	0.32	0.83	0.20	0.37	0.81
Na ₂ O	0.02	0.02	0.01	0.01	0.01	0.01	0.01	0.01	0.02
K ₂ O	0.01	0.01	0.01	0.01	0.01	0.01	0.01	0.01	0.01
P ₂ O ₅	0.01	0.01	0.02	0.01	0.01	0.01	0.01	0.02	0.01
LOI	6.80	6.20	7.86	7.10	7.65	6.34	6.76	6.47	5.53
Total	99.64	99.01	100.03	99.80	99.15	99.13	99.32	99.70	99.62
Ag	0.01	0.01	0.02	0.01	0.01	0.03	0.02	0.02	0.01
As	0.5	0.5	1.3	0.5	0.5	0.5	0.5	2.5	0.5
Ba	1	0.7	11.8	0.5	2.6	0.4	5.9	2.8	1.9
Be	0.2	0.2	0.2	0.2	0.2	0.2	0.2	0.2	0.2
Bi	0.1	0.1	0.1	0.1	0.1	0.1	0.1	0.1	0.1
Cd	0.05	0.05	0.05	0.05	0.05	0.05	0.06	0.05	0.05
Co	95.8	100.3	111.7	92.5	103.3	90.9	93.3	85.5	88.1

Rock type	Dunite	Dunite	Harzburgite	Harzburgite	Harzburgite	Harzburgite	Lherzolite	Lherzolite	Lherzolite
Cr	23	616	955	1009	858	924	2239	1608	871
Cs	0.1	0.1	0.1	0.1	0.1	0.1	0.1	0.1	0.1
Cu	0.7	1.4	7.7	2.8	3.2	3.7	25.7	25.9	17
Hg	0.05	0.05	0.05	0.05	0.05	0.05	0.05	0.05	0.05
In	0.01	0.01	0.01	0.01	0.01	0.01	0.01	0.01	0.01
Li	0.5	1	2.3	0.5	0.5	0.7	1.7	2.9	4.1
Mo	0.3	0.3	0.4	0.3	0.4	0.2	0.4	0.3	0.2
Nb	0.5	0.5	0.5	0.5	0.5	1.2	0.5	0.5	0.5
Ni	2217.3	2134.1	2666.2	1948.7	2165.3	1945	1855.5	2047.8	1843.2
Pb	0.4	0.2	0.2	0.2	0.2	0.2	0.2	0.3	0.2
Rb	0.1	0.1	0.1	0.2	0.1	0.1	0.1	0.3	0.1
Re	0.01	0.01	0.01	0.01	0.01	0.01	0.01	0.01	0.01
S	198	850	59	138	60	174	101	50	554
Sb	0.1	0.1	0.1	0.1	0.1	0.1	0.1	0.1	0.1
Sc	2	6	8	8	8	7	11	9	6
Se	0.34	0.05	0.05	0.11	0.08	0.06	0.08	0.13	0.09
Sn	0.2	0.2	0.2	0.2	0.2	0.2	0.2	0.2	0.2
Sr	1.6	0.8	10.1	0.9	25.7	1.5	5.8	2.8	5.2
Te	0.2	0.2	0.2	0.2	0.2	0.2	0.2	0.2	0.2
Th	0.02	0.02	0.02	0.02	0.02	0.04	0.02	0.11	0.02
Tl	0.1	0.1	0.1	0.1	0.1	0.1	0.1	0.1	0.1
U	0.02	0.02	3.71	0.02	0.02	0.02	0.02	0.29	0.03
V	36	45	71	59	58	60	96	80	63
W	0.1	0.1	0.1	0.1	0.1	0.1	0.1	0.1	0.1
Y	0.05	0.05	0.23	0.28	0.05	0.64	1.49	1.09	0.45
Zn	25.9	27.5	39.5	25.6	24.2	26	42.6	35.8	30.2
Zr	1	1	1	1	1	1	1	2	1
Ce	0.05	0.06	0.21	0.3	0.07	0.18	0.13	1.27	0.26
Dy	0.02	0.02	0.05	0.04	0.02	0.03	0.28	0.19	0.18
Er	0.05	0.05	0.05	0.05	0.05	0.05	0.23	0.15	0.16
Eu	0.02	0.02	0.02	0.02	0.02	0.02	0.03	0.06	0.02
Gd	0.05	0.05	0.06	0.05	0.05	0.05	0.16	0.16	0.11
Ho	0.02	0.02	0.02	0.02	0.02	0.02	0.08	0.05	0.05
La	0.05	0.05	0.17	0.18	0.05	0.08	0.06	0.94	0.08
Lu	0.02	0.02	0.02	0.02	0.02	0.02	0.04	0.03	0.03
Nd	0.02	0.04	0.24	0.14	0.04	0.11	0.14	0.68	0.14
Pr	0.05	0.05	0.05	0.05	0.05	0.05	0.05	0.17	0.05
Sm	0.02	0.02	0.05	0.02	0.02	0.02	0.07	0.13	0.04
Tb	0.02	0.02	0.02	0.02	0.02	0.02	0.04	0.04	0.02
Tm	0.05	0.05	0.05	0.05	0.05	0.05	0.05	0.05	0.05
Yb	0.05	0.05	0.07	0.07	0.05	0.06	0.28	0.19	0.2

Petrography of dunites

Dark green in colour, the fractured dunites occur in the southern and southeastern parts of the Dare Kaftor village (Fig. 4A), consisting of mainly olivine (>90%) with opaque minor minerals like chrome-spinel (Fig. 5A). They show sieve texture formed due to alteration of olivine to serpentine (Fig. 5B). The olivine has had been converted to a series of iron oxides, clay minerals (iddingsite) due to the intense alteration.

Petrography of harzburgites

Forming the largest part of the peridotite section, green to dark green in colour, fractured and faulted, these rocks have

also been lateralized at varying degrees, in some areas, like Gashur (east of Haft Cheshmeh) where its great mass is covered by Miocene limestones and basalts (Fig. 4B). Asbestos veins occur in it with coarse crystals of bronzite (Fig. 4C). They are composed of olivine (50-60%), orthopyroxene (30-40%) and chrome-spinel (10-15%) with granular and sieve textures. Orthopyroxenes are in the form of bronzite, which show less alteration (Fig. 6A) except along the altered fractures/bastitic parts. The orthopyroxenes show undulose extinction- a sign of tectonic activity. Chrome-spinel shows anhedral-euhedral crystal due to tectonic activity with serpentinized fractures, filled with chrysotile asbestos (Fig. 6B).

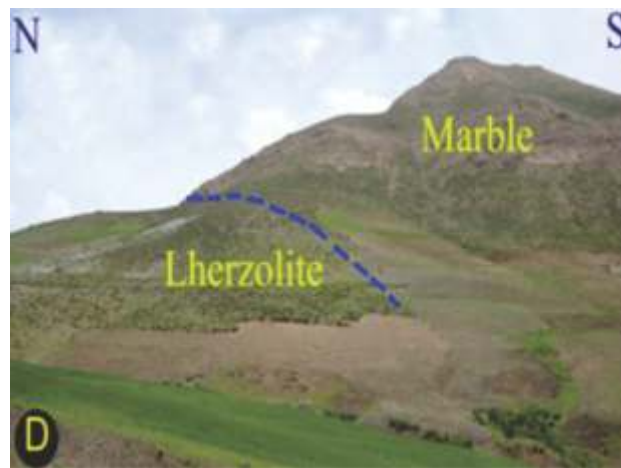
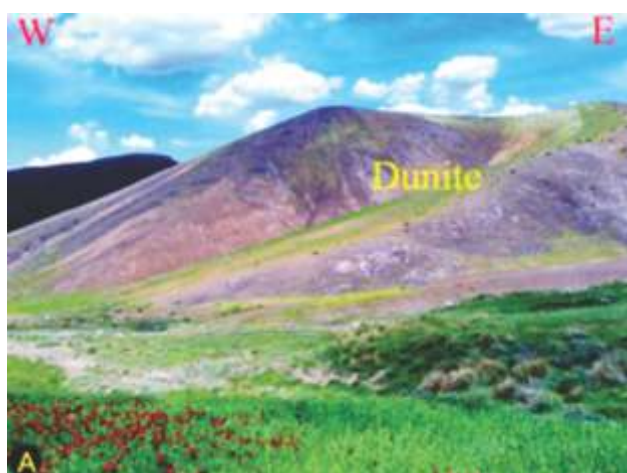


Fig. 4: A- Dunite mass in the eastern part of Noorabad. B- Harzburgite mass in Gashur that covered by miocene limestones. C- Bronzite minerals with the special brightness in the harzburgite rocks of Gashur. D- The faults boundary between the lherzolite masses and the marble in the study area.

Petrography of lherzolites

The lherzolite masses may be seen in two forms: the first in the form of marginal masses with gradual boundaries with harzburgite, is the most common of all lherzolite in the margin of the western harzburgite masses of the Dare Kaftar village (35km to Noorabad-Harsin road); while the second forms separate masses of lherzolites, which occur north of the Melekabud village (northwest of Noorabad) with a fault boundary along the marble. These peridotites are seen as melange with gababro and diabasic dikes. Here alteration is more intense than the previous one. Megascopically

lherzolite varies in shades of green to dark green showing intense tectonic effects of faulting (slickenside, visible (Fig 4D).

These rocks contain olivine minerals (10-15%), orthopyroxene (50-40%) (Fig. 5 A & B), clinopyroxene (40- 300%) (Fig. 6), chrome-spinel (less than 5%, %) and show granular and sieve textures. Olivine has been extensively altered into serpentine. Orthopyroxenes are surrounded by fine-grained clinopyroxenes as porphyroblast (Fig. 7A) with inclusions of clinopyroxene (Fig. 7AB).

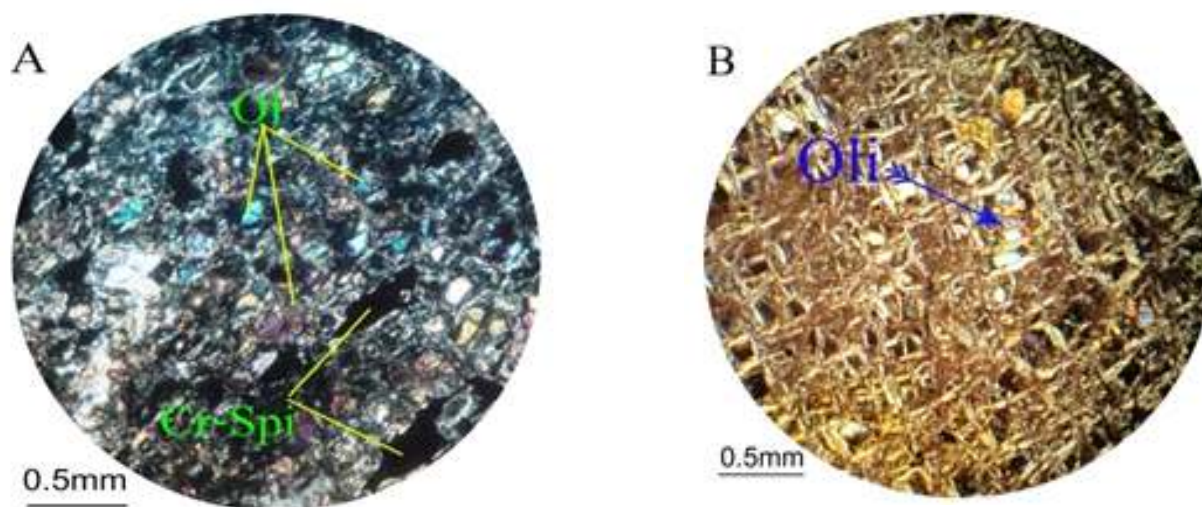


Fig. 5: A- Olivine minerals in dunite with sieve texture in the southeastern dunites of the Dare Kaftar village. B- The remaining olivine minerals in dunite with sieve texture (xpl light).

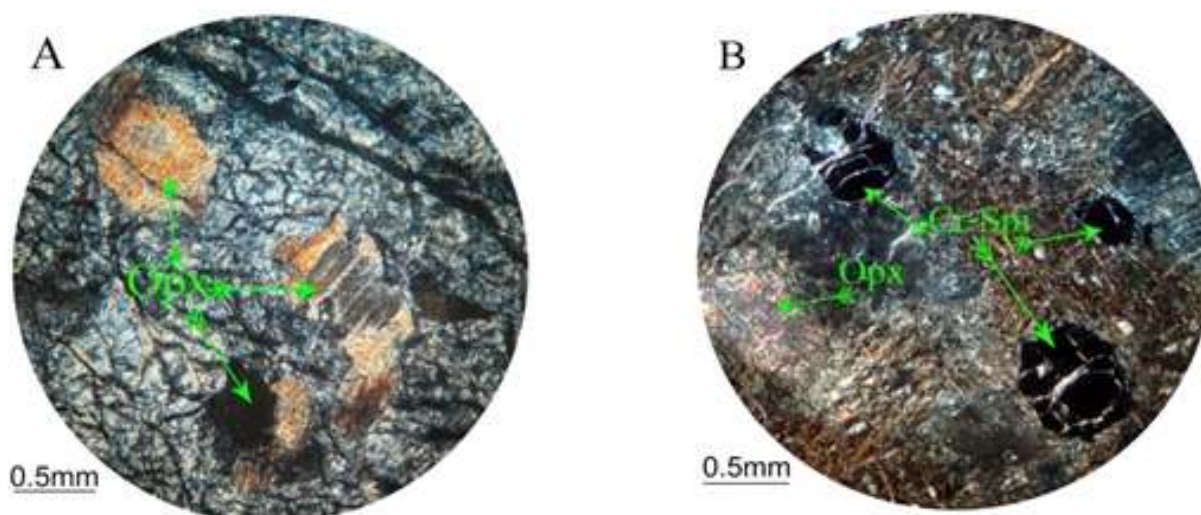


Fig. 6: A- Orthopyroxene with undulose extinction, in the background of serpentine resulting from olivine alteration with a sieve texture. B- Broken crystals of chrome-spinel with residual orthopyroxene mineral in the background of vein adenozeite and asbestos (xpl light).

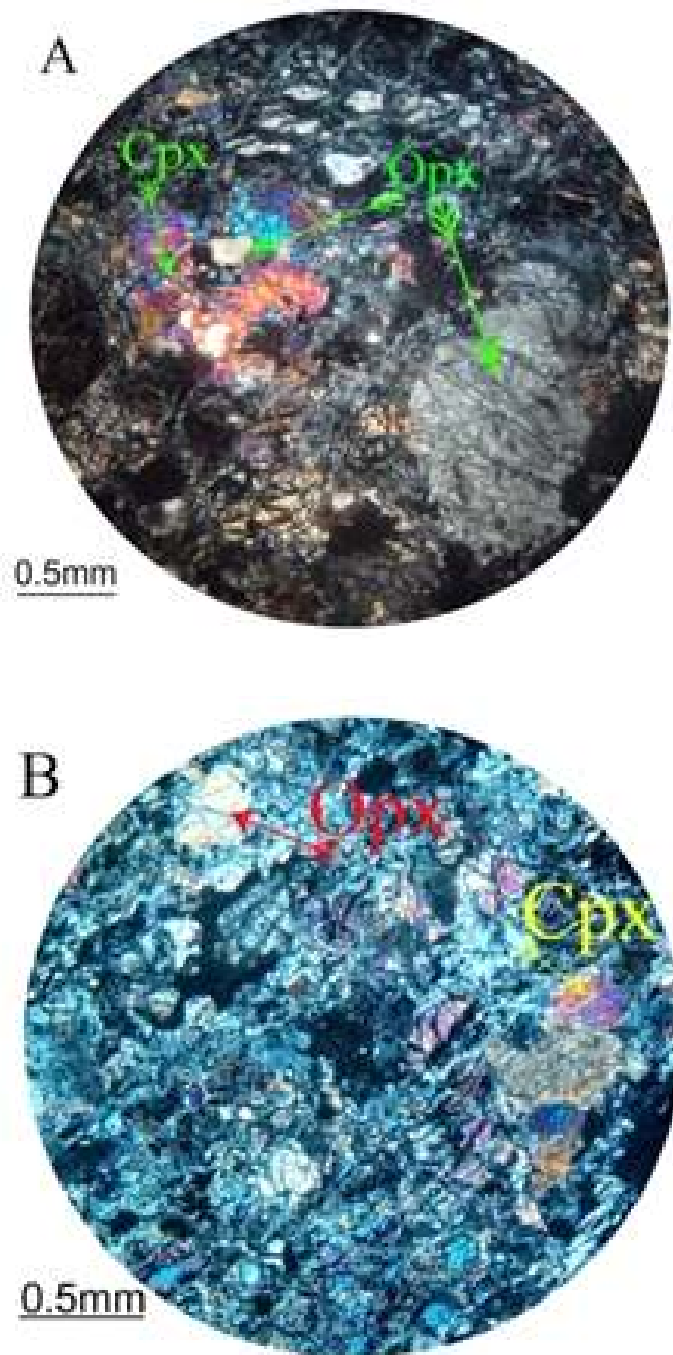


Fig.7: A- Orthopyroxene inclusion in clinopyroxene, B- Lherzolite with clinopyroxene microcrystalline that has sieve texture (xpl light).

Geochemistry

The highest amount of magnesium occurs in dunites (Fig. 8). In the diagrams of magnesium versus the main elements, it is observed that although serpentine alteration affected in the dispersal of samples around the regression line, but in general, with the advancement of magma differentiation, first the compatible elements (with a smaller ion radius, such as magnesium), entered into olivine, then incompatible elements that entered in the magma by reducing the amount of magnesium during subtraction (Fig. 9).

In the pattern of the incompatible elements pattern versus the primary mantle diagram dunites are depleted of incompatible elements and have negative slope of LILE to HFSE. Also, these peridotites have positive anomalies in LILE elements such as Cs, U, K, Pb and P, and in HFSE such as Ce, Nd and Y. (Fig. 10A). The pattern of REE elements versus chondrites in these dunites show a positive slope from LREE to HREE with depletion in Dy and Yb and positive anomalies in Tm (Fig. 10B)

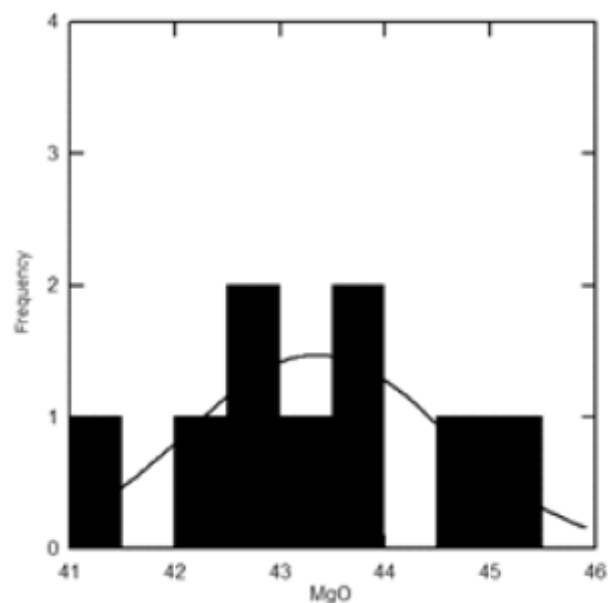


Fig. 8: Frequency of magnesium in the peridotites of the study area.

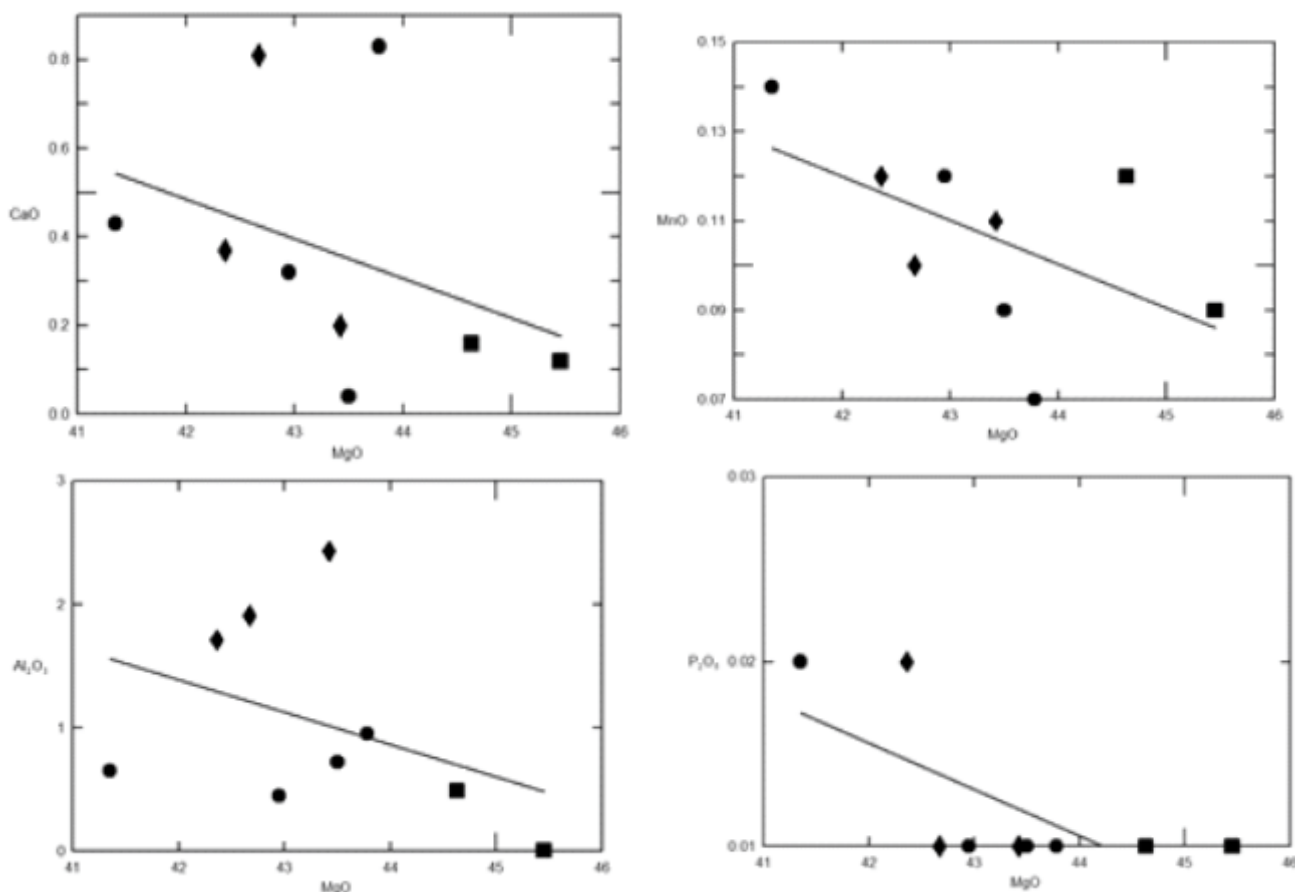


Fig. 9: Magnesium versus the main elements diagrams. Solid circles. dunite; solid squares. harzburgite ; solid diamond. lherzolite.

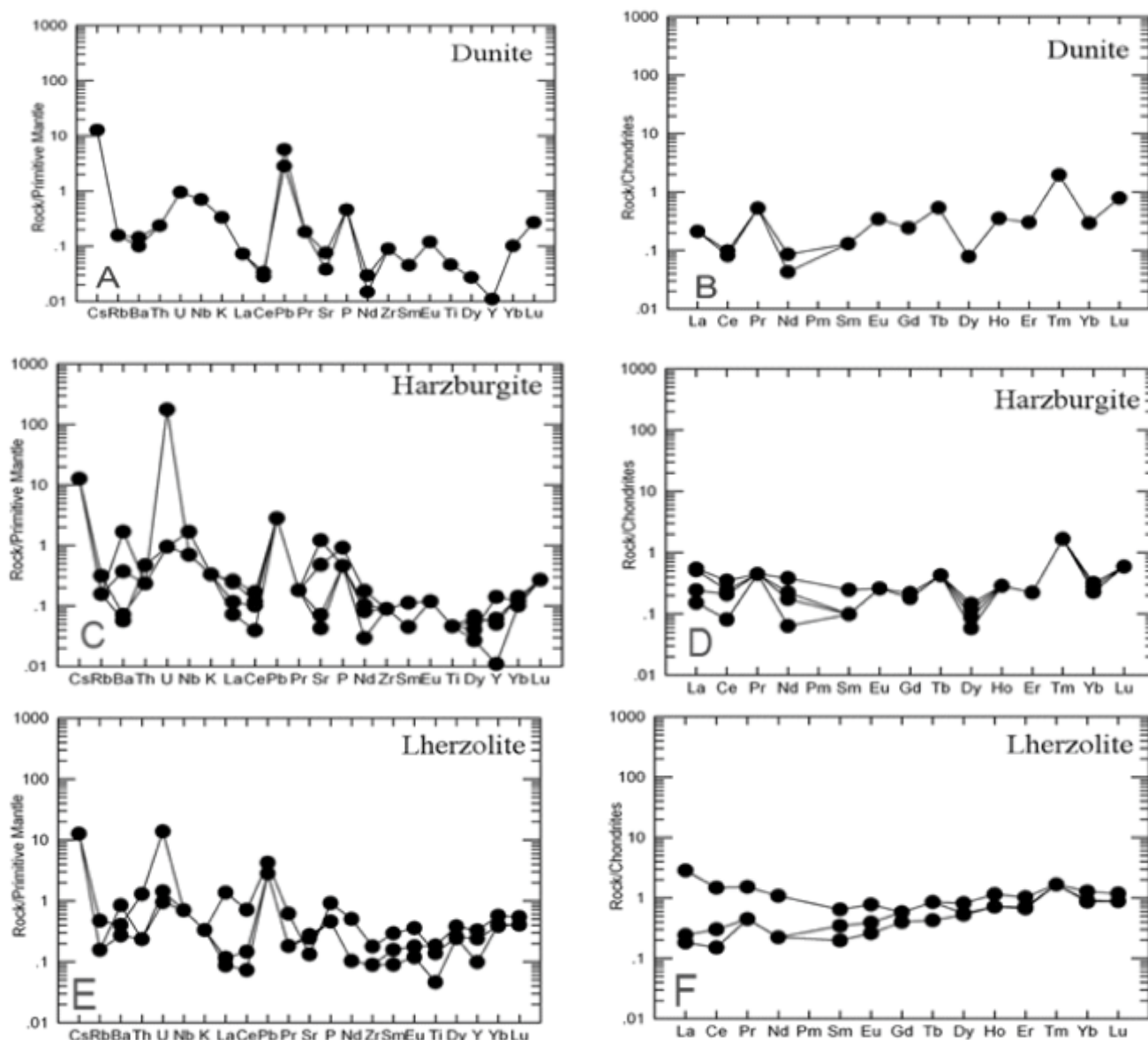


Fig. 10: A- Distribution pattern of dunite rare elements versus the primary mantle composition, B- Distribution pattern of dunite rare elements versus chondrite composition, C- Distribution pattern of harzburgite trace elements versus primary mantle composition, D- Distribution pattern of harzburgite trace elements versus the chondrite composition, E- Distribution pattern of lherzolite trace elements versus primary mantle composition, F- Distribution pattern of lherzolite trace elements versus the chondrite composition (Sun & Mc Donough, 1989).

In the normalized pattern of the incompatible elements of the harzburgites versus the mantle, diagram, like the dunites are depleted in incompatible elements, and has a negative slope of incompatible light and HFSE. But they have a lower HFSE than lherzolites (Fig. 10 C). These rocks have the positive anomaly of the LILE elements such as Cs, U, Pb, P and Ba, which can be attributed to the effect of molten material or the released fluids from the subducted plate. Although they have depleted from Ba and Sr (samples S-1 and S-31, relative to N-4 and NK36) as also found by Kiani

et al. (2015) and Tahmasebi *et al.* (2016). But, the effect of intensity alteration in these patterns should not be considered ineffective. Harzburgite peridotites are highly depleted from REE elements and show almost a 'flat pattern' in the chondrite normalized diagram (Fig. 10D) and have a positive anomaly in Tm like lherzolites) and negative anomalies in Dy and Yb (unlike lherzolites), which may be attributed to different degrees of partial melting of these peridotites (Fig. 11 A and B).

Lherzolites in the normalized pattern versus the primary

mantle, have a negative slope of LILE to high field strength elements (HFSE), and have positive abnormalities in Cs, U, Pb and P and negative abnormalities in Zr, Ti and Y (Fig. 10E). These rocks in the normalized pattern versus chondrite have depletion in all REEs with a negative slope from HREE to LREE, however, in the sample S-7, there is more depletion in MREE elements (Fig. 10F). The high volume of HREE in these peridotites are associated with a high presence of clinopyroxene (a mineral susceptible to HREE acceptance).

Mantle melting percentage

To obtain the melting percentage of peridotites, we used Yb-Sc logarithmic diagram or the logarithmic diagram of Yb-V (Pearce & Parkinson, 1993) (Fig. 11-A and B). Accordingly, lherzolites 5-10% and harzburgites with dunites have tolerated 15-20% melting. The Yb-V diagram is also proposed for obtaining oxygen fugacity during melting (Pearce and Parkinson, 1993; Melcher *et al.*, 2002). This figures show high fO_2 , than MORB, which indicates that the peridotites of this region are related to the peridotites of the SSZ region and, in this respect, are similar to the Na'in ophiolites and peridotites (Shafaii Moghadam *et al.*, 2009).

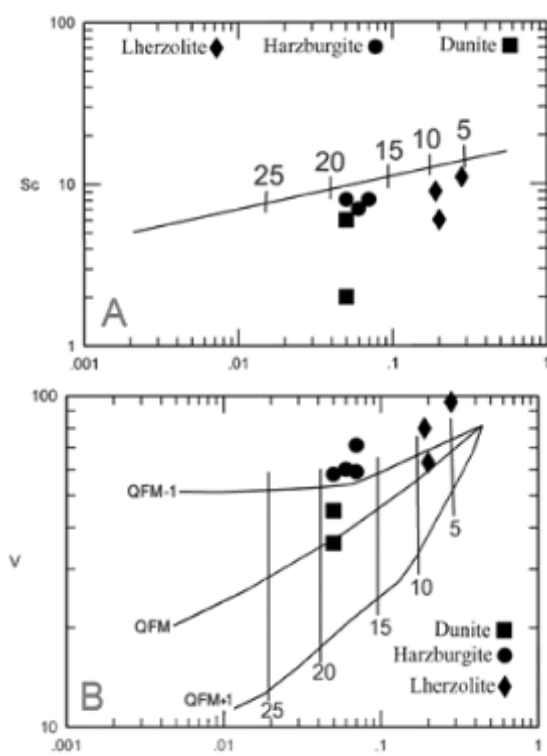


Fig. 11: A- Yb-Sc logarithmic diagram (Pearce & Parkinson, 1993), that show 5-10% melting for lherzolites and 15-20% for harzburgites with dunites. **B-** The logarithmic diagram of Yb-V (Pearce & Parkinson, 1993), which show lherzolites and harzburgites with dunites tolerate 5-10% and 15-20% melting respectively, and the oxygen fugacity during melting is high and relevant to subduction areas.

Conclusion

The major volume of Noorabad ophiolite as part of Kermanshah, western Iran, consists of peridotitic rocks, like dunite, harzburgites and lherzolites, consisting of olivine, pyroxene and chrome-spinel that have been converted into serpentine minerals and iron oxides. The bronzite mineral is the most abandoned ferromagnesian mineral in these rocks, which can be seen in manual samples. These rocks are depleted in incompatible elements and show negative slope of incompatible light elements to HFSE. These rocks in the normalized pattern versus chondrite are depleted in REE with a negative slope of HREE to LREE. Values of HREE in lherzolites than dunites and harzburgites can also be associated with a high percentage of clinopyroxene presence, and lower melting rate of this lherzolites. The melting percentage of studied peridotites indicates a high fO_2 than MORB, which indicates that the peridotites of this region are related to the peridotites of the SSZ region of the Neo-Tethys Ocean.

References

- Agard P. Omrani L. Jolivet L. and Mouthereau F.(2005): Convergence history across Zagros (Iran): constraints from collisional and earlier deformation. *International Journal of Earth Sciences (Geologische Rundschau)*, 94, 401–419.
- Arvin M. (1990): Petrology and geochemistry of ophiolites and associated rocks from the Zagros suture, Neyriz, Iran. (In *Ophiolites, Oceanic Crustal Analogues. Proceedings of the Symposium "Troodos 1987"* (Eds.: Malpas, J., Moores, E.M., Panayiotou, A., Xenophontos, C.) The Geological Survey Department, Nicosia, Cyprus, pp. 351–365.
- Dilek Y. and Thy P. (2009): Island arc tholeiite to boninitic melt evolution of the Cretaceous Kizildag (Turkey) ophiolite : model for multi-stage early arc– forearc magmatism in Tethyan subduction factories. *Lithos*, 113, 68–87.
- Dilek Y. and Delaloye M. (1992): Structure of the Kizildag ophiolite, a slow-spread Cretaceous ridge segment north of the Arabian promontory. *Geology* 20, 19-22.
- Dilek Y. Furnes H. and Shallo M. (2007): Suprasubduction zone ophiolite formation along the periphery of Mesozoic Gondwana. *Journal of Gondwana Research* 11, 453-475.
- Ghazi A.M. and Hassanipak A.A. (1999): Geochemistry of subalkaline and alkaline extrusives from the Kermanshah ophiolite, Zagros Suture Zone, western Iran: implications on Tethyan plate tectonics. *Journal of Asian Earth Sciences* 17: 319-332.

- Goodenough K.M. Style M.T. Schofield D.I. Thomas R. J. Crowley Q. C. Lilly R. M. Mckerverey J. Stephenson D. and Carne J. N. (2010): Architecture of the Oman–UAE ophiolite : evidence for a multi-phase magmatic history. *Arabian Journal of Geosciences*, 3, 439–458.
- Hassanipak A.A. and Ghazi A.M. (2000): Petrology, geochemistry and tectonic setting of the Khoy ophiolite , northwest Iran: implications for Tethyan tectonics. *Journal of Asian Earth Sciences* 18, 109–121.
- Hébert R. Serri G. and Hekinian R. (1989): Mineral chemistry of ultramafic tectonites and ultramafic to gabbroic cumulates from the major oceanic basins and Northern Apennine ophiolite s (Italy): a comparison. *Chemical Geology* 77, 183–207.
- Kiani M. (2011): Geochemistry, economic geology and petrogenesis of the ophiolite complex in the Alashtar-Kermanshah axis. MSc thesis, Islamic Azad University, Khorramabad Branch, Iran (in Persian).
- Kiani M. Ahmadi-Khalaji A. Kamali Z. and Shafaii Moghadam H. (2015): Geochemistry of diabasic dikes and andesitic-basaltic lavas in Noorabad-Kermanshah ophiolite *Journal of Tethys*: Vol. 3, No. 1, 1–15.
- Malpas J. Zhou M.-F. Robinson P.T. and Reynolds P.H. (2003): Geochemical and geochronological constraints on the origin and emplacement of the Yarlung Zangbo ophiolites, Southern Tibet. In: Dilek Y. Robinson P.T. (Eds.), *Ophiolites in Earth History*. Geological Society of London Special Publication, vol. 218, pp. 191–206.
- Mukasa S. and ludden J.N. (1987): Uranium–lead isotopic ages of plagiogranites from the Troodos ophiolite , Cyprus, and their tectonic significance. *Geology*, 15, 825–828.
- Parlak O. Hoeck V. Kozlu H. and Delaloye M. (2006): Oceanic crust generation in an island arc tectonic setting, SE Anatolian Orogenic Belt (Turkey). *Geological Magazine* 141, 583–603.
- Pearce J. A. and Parkinson I. J. (1993): Trace element models for mantle melting: application to volcanic arc petrogenesis. In: Prichard H. Malabaster. T. Harris N.B. Neary C. R. (Eds.), *Magmatic Processes and Plate Tectonics*. Geological Society of London, Special Publication, 79, 373–403.
- Pearce J.A. Lippard S.J. and Roberts S. (1984): Characteristics and tectonic significance of supra-subduction zone ophiolites. In: Kokelaar B.P. Howells M.F. (Eds.) *Marginal Basin Geology*, Blackwell Scientific; Geological Society Special Publication 16, 77–94.
- Robinson P.T. and Malpas J. (1990): The Troodos ophiolite of Cyprus: new perspectives on its origin and emplacement. In: Malpas J. Moores E.M. Panayiotou A. Xenophontos C. (Eds.), *Ophiolite s, Oceanic Crustal Analogues*. Proceedings of the Symposium “Troodos 1987”. The Geological Survey Department, Nicosia, Cyprus, 13–26.
- Shafaii Moghadam H. and Stern R. J. (2011): Geodynamic evolution of Upper Cretaceous Zagros ophiolite s: formation of oceanic lithosphere above a nascent subduction zone. *Geological Magazine*, 148, 762–801, doi:10.1017/S0016756811000410
- Shafaii Moghadam H. Stern R. J. Kimura J.I. Hirahara Y. Senda R. and Miyazaki T. (2012): Hf-Nd Isotopic Constraints on the Origins of Zagros Ophiolite s. *The Island Arc*, 21, 202–214, doi: 10.1111/j.1440-1738.2012.00815.x.
- Shafaii Moghadam H. Whitechurch H. Rahgoshay M. and Monsef I. (2009): Significance of Nain-Baft ophiolitic belt (Iran): short-lived, transtensional Cretaceous back-arc oceanic basins over the Tethyan subduction zone. *Comptes Rendus Geosciences*, 341, 1016–28, doi: 10.1016/j.crte.2009.06.011.
- Shafaii Moghadam H. Corfu F. and Stern R. (2013): U-Pb zircon ages of Late Cretaceous Nain-Dehshir ophiolite s, central Iran. *Journal of the Geological Society of London* 170, 175–184. doi: 10.1144/jgs2012-066.
- Stocklin J. (1977): Structural correlation of the Alpine range between Iran and Central Asia. *Mémoire Hors-Serie, Société Géologique de France* 8: 333–353.
- Sun S.S. and McDonough W.F. (1989): Chemical and isotopic-systematics of oceanic basalts: implications for mantle composition and processes. In: Saunders, A.D., Norry, M.J. (Eds.), *Magmatism in the Ocean Basins*. Geological Society of London Special Publication 42: 313–345.
- Tahmasbi Z. Kiani M. and Ahmadi-Khalaji A. (2016): Petrology and Geochemistry of Diabasic Dikes and Andesitic-Basaltic Lavas in Noorabad-Harsin Ophiolite, SE of Kermanshah, Iran. *Journal of Earth Science*, 27(6), 935–944.
- Warren C. J. Parrish R. R. Waters. D. J. and Searle M.P. (2005): Dating the geologic history of Oman's Semail ophiolite: insights from U–Pb geochronology. *Contributions to Mineralogy and Petrology*, 150, 403–422.